

Kertesz on Fat Graphs?

W. Janke

Institut für Theoretische Physik
Universität Leipzig
Augustusplatz 10/11
D-04109 Leipzig, Germany

and

D.A. Johnston and M. Stathakopoulos

Dept. of Mathematics
Heriot-Watt University
Riccarton
Edinburgh, EH14 4AS, Scotland

February 6, 2008

Abstract

The identification of phase transition points, β_c , with the percolation thresholds of suitably defined clusters of spins has proved immensely fruitful in many areas of statistical mechanics. Some time ago Kertesz suggested that such percolation thresholds for models defined *in field* might also have measurable physical consequences for regions of the phase diagram below β_c , giving rise to a “Kertesz line” running between β_c and the bond percolation threshold, β_p , in the M, β plane.

Although no thermodynamic singularities were associated with this line it could still be divined by looking for a change in the behaviour of high-field series for quantities such as the free energy or magnetisation. Adler and Stauffer did precisely this with some pre-existing series for the regular square lattice and simple cubic lattice Ising models and did, indeed, find evidence for such a change in high-field series around β_p . Since there is a general dearth of high-field series there has been no other work along these lines.

In this paper we use the solution of the Ising model in field on planar random graphs by Boulatov and Kazakov to carry out a similar exercise for the Ising model on random graphs (i.e. coupled to 2D quantum gravity). We generate a high-field series for the Ising model on Φ^4 random graphs and examine its behaviour for evidence of a Kertesz line.

1 Introduction

The question of how to give a geometrical, percolation-like interpretation of the thermal transition in the Ising model was finally resolved by Coniglio and Klein [1], although the idea is already implicit in the work of Fortuin and Kasteleyn [2] on a correlated bond-percolation model for the q -state Potts model and in many ways is a realisation of Fisher's earlier ideas on critical droplets [3]. The key insight was to construct spin clusters in which like spins were joined with probability $p = 1 - \exp(-2\beta)$, where $\beta = 1/k_B T$ is the inverse temperature. These then percolated at the correct critical temperature T_c and gave the correct thermal exponents. The definition of such stochastic clusters has led directly to the development of cluster algorithms and similar geometrical representations in many statistical mechanical models.

Since Coniglio-Klein clusters are intended to access the thermal phase transition of the Ising model they are not usually formulated in the presence of an external field, since in this case the free energy becomes analytic and the thermal transition is washed out. However it is clear that one can still build such clusters when the external field is non-zero. For a given external field value H these clusters will percolate at some temperature $T_K(H)$, and varying H then traces out the so-called Kertesz line shown in Fig. 1 in the M, u plane, where M is the magnetisation and $u = \exp(-4\beta)$. For $H = 0$ we have the usual thermal Ising transition at u_c , whereas for $H \rightarrow \infty$ we recover standard bond percolation for the lattice in question at u_p .

Although a percolative transition exists across the Kertesz line no singularities are expected in the thermodynamic quantities related to the Ising model, since these can only appear for $H = 0$. Nonetheless, something physical is going on since the percolative transition is signalled by “wrong-sign”, say down, spin clusters losing their surface tension. This begs the question of whether the Kertesz line leaves any discernible signal in measurable quantities. This issue was discussed by Kertesz himself [4], and later investigated numerically by Stauffer and Adler [5]. If one considers the number of down spin clusters $n_s(u, H)$ in a non-zero up field H then standard nucleation theory leads to

$$\log n_s(u, H) = s \log y - s^\sigma \Gamma \quad (1)$$

below the Kertesz line, where $y = \exp(-2H)$ and $\sigma = 1 - 1/d$. The second term arises from the surface tension Γ of the droplets and is a direct extrapolation of the $H = 0$ ($y = 1$) result. On the other hand above the Kertesz line a zero surface tension expression of the form

$$\log n_s(u, H) = s \log y + s \log \lambda(u, H) \quad (2)$$

where $\lambda < 1$ is postulated. This means that cluster numbers will decay as

$$n_s = \exp(-\Gamma s^{1-1/d}) y^s \quad (3)$$

below the Kertesz line whereas they will decay as $y^s \lambda^s$ above the line.

Physical quantities such as the magnetisation can be expressed in terms of n_s ,

$$M = 1 - 2 \sum_s s n_s(u, H), \quad (4)$$

so we can see that they can be expressed in terms of a (large-field) expansion in y using eqs. (1) and (2). Since equ. (2) shows that y is effectively replaced by $y\lambda$ above the Kertesz line, one might expect the series for M (and others) to converge up to some $y > 1$ (since $\lambda < 1$).

2 Square Lattice Reprise

In order to investigate the possible consequences of a Kertesz line Adler and Stauffer [5] analysed the radius of convergence of some long-standing high-field series for the free energy and the magnetisation of the Ising model using Padé approximants [6]. We briefly review their results here for comparison with the random graphs in the next section. Taking the series for the free energy F or its derivative, we have

$$\begin{aligned} F &= \sum_s L_s(u) y^s, \\ \frac{dF}{dy} &= \sum_s s L_s(u) y^{s-1}, \end{aligned} \quad (5)$$

where the so-called high-field polynomials $L_s(u)$ were calculated up to order 15 for the square lattice in [6].

The series for F , $\frac{dF}{dy}$ and the magnetisation M were subjected to a standard unbiased Dlog-Padé analysis in order to estimate the radius of convergence. If we assume a singularity of the form $F \sim (y - y_c)^{-\lambda}$, then

$$\frac{d}{dy} \log F = -\frac{\lambda}{y - y_c} \quad (6)$$

and an $[L/M]$ Padé approximant to $\frac{d}{dy} \log F$ (or $\frac{dF}{dy}$, or M),

$$[L/M] = \frac{P_L(y)}{Q_M(y)} = \frac{p_0 + p_1 y + \dots + p_L y^L}{q_0 + q_1 y + \dots + q_M y^M}, \quad (7)$$

would be expected to show the pole at y_c as a zero of $Q_M(y)$. For the square lattice for instance $u_c = 3 - 3\sqrt{2} = 0.17157\dots$ and $u_p = 1/4$, so we would expect to see a change in y_c at, or around, u_p .

We show the results of such an analysis on $\frac{dF}{dy}$ for the estimated radius of convergence as a function of u in Fig. 2. We can see that there is evidence for a change in the behaviour of y_c around $u = 1/4$. In the plotted data jumps are present in the $[7/7]$ and $[6/7]$ approximants at u_p , and the $[5/5]$ and $[6/6]$ approximants cease to give a real pole term for some $u \sim u_p$. In Fig. 2 we have plotted the $[5/5]$ and $[6/6]$ approximants up to the largest real pole value obtained. As shown in [5] the behaviour for other approximants and for F and M is similar – in all cases there is evidence of an increase in the estimated y_c around $u = 1/4$ or the approximant's estimates of y_c become complex.

One detail that should be noted is that both here and in the random graph case investigated below there is a tendency for the approximants to throw up spurious cancelling

pole/zero pairs, so one must be careful to look at both the numerator and denominator of the approximant to make sure that one is determining the “real” pole term. This also introduces a certain degree of subjectivity into proceedings since the poles and zeroes are only equal to within numerical accuracy. All the series calculations were done with *exact* arithmetic, with fixed (but large) precision only being resorted to in the final stage of obtaining the roots of the Padé numerators and denominators.

An analysis of the series for the simple cubic lattice Ising model, available up to order 13, in [5] also gave very similar results, with signs of an increase in the estimated radius of convergence, or instability in the approximants, in the vicinity of the percolation temperature for the lattice. The usual caveats of course apply to any such discussion, since the series involved are quite short (and of some considerable vintage), but the cumulative evidence of the various approximants and the results on different lattices was felt in [5] to lend support to the Kertesz scenario.

3 Fat Random Graphs

Given the evidence for a Kertesz line in the Ising model on the square and cubic lattices it is tempting to look elsewhere for the phenomenon. In order to carry out such an analysis for other models (or lattices) we require a high-field expansion, which are in general rather hard to come by. In what follows we discuss obtaining such an expansion for an exact solution to the Ising model *in field* on planar (fat) random graphs which was derived by Boulatov and Kazakov [7, 8]. They considered the partition function for the Ising model on a single planar graph with n vertices

$$Z_{\text{single}}(G^n, \beta, H) = \sum_{\{\sigma\}} \exp \left(\beta \sum_{\langle i,j \rangle} G_{ij}^n \sigma_i \sigma_j + H \sum_i \sigma_i \right), \quad (8)$$

then summed it over some suitable class $\{G^n\}$ of n vertex graphs (e.g. Φ^3 or Φ^4 random graphs) resulting in

$$Z_n = \sum_{\{G^n\}} Z_{\text{single}}(G^n, \beta, H), \quad (9)$$

before finally forming the grand-canonical sum over differently sized graphs

$$\mathcal{Z} = \sum_{n=1}^{\infty} \left(\frac{-4gc}{(1-c^2)^2} \right)^n Z_n, \quad (10)$$

where $c = u^{1/2} = \exp(-2\beta)$. This last expression could be calculated exactly as matrix integral over $N \times N$ Hermitian matrices,

$$\mathcal{Z} = -\log \int \mathcal{D}\phi_1 \mathcal{D}\phi_2 \exp \left(-\text{Tr} \left[\frac{1}{2}(\phi_1^2 + \phi_2^2) - c\phi_1\phi_2 - \frac{g}{4}(e^H\phi_1^4 + e^{-H}\phi_2^4) \right] \right), \quad (11)$$

where the $N \rightarrow \infty$ limit is to be taken to pick out the planar diagrams and we have used the potential appropriate for Φ^4 (4-regular) random graphs.

When the integral is carried out the solution is given by

$$\mathcal{Z} = \frac{1}{2} \log \frac{z}{g} - \frac{1}{g} \int_0^z \frac{dt}{t} g(t) + \frac{1}{2g^2} \int_0^z \frac{dt}{t} g(t)^2, \quad (12)$$

where the function $g(z)$ is

$$g(z) = 3c^2 z^3 + z \left[\frac{1}{(1-3z)^2} - c^2 + \frac{3z(y^{1/2} + y^{-1/2} - 2)}{(1-9z^2)^2} \right]. \quad (13)$$

As we can see this is a solution in field for the Ising model on random graphs, since $g(z)$ has been obtained in full generality for $y = \exp(-2H) \neq 1$.

In order to generate a high-field series from equ. (12) we revert the series for $g(z)$ to get a series $z(g)$. This can then be used in equ. (12) in order to obtain an expansion for the partition function in powers on g (i.e. in the number of vertices). As we noted in [9] it is only necessary to consider the first of the terms in $\mathcal{Z} = \mathcal{Z}_1 + \mathcal{Z}_2 + \mathcal{Z}_3$ with

$$\begin{aligned} \mathcal{Z}_1 &= \frac{1}{2} \log \frac{z}{g}, \\ \mathcal{Z}_2 &= -\frac{1}{g} \int_0^z \frac{dt}{t} g(t), \\ \mathcal{Z}_3 &= \frac{1}{2g^2} \int_0^z \frac{dt}{t} g(t)^2, \end{aligned} \quad (14)$$

since $\mathcal{Z}_k = \sum_n a_k^n A_n(u) g^n$ where $A_n(u)$ is *identical* for all the \mathcal{Z}_k .

This can be traced back to the generic expression for the partition function of any Hermitian matrix model, which is of the form

$$\mathcal{Z} = \int_0^1 d\xi (1-\xi) \log(f(\xi)) + \dots, \quad (15)$$

where in the case of the Ising model on Φ^4 graphs f is the solution to

$$g\xi = \left(\frac{2gf}{c} \right) \left(\frac{1}{(1 - \frac{6gf}{c})^2} - c^2 + \frac{6gf}{c} \frac{(y^{1/2} + y^{-1/2} - 2)}{(1 - 9(\frac{2gf}{c})^2)^2} \right) + 3c^2 \left(\frac{2gf}{c} \right)^3. \quad (16)$$

The expression in equ. (12) is obtained from this by defining $z = 2gf/c$ and integrating by parts. One finds that the coefficient of g^n in \mathcal{Z}_1 should be $(n+1)(n+2)$ times the full value obtained from expanding $\mathcal{Z}_1 + \mathcal{Z}_2 + \mathcal{Z}_3$ from these considerations, which can be confirmed by comparison with the results presented for low orders in [10, 11]. For example, the coefficient of \tilde{g}^2 in [10] is found to be¹

$$(1/8)c^{-2}y^{-1}[9 + (16c^2 + 2c^4)y + 9y^2], \quad (17)$$

which is

$$12 \times \mathcal{Z}_1 = 12 \times (3/2)c^{-2}y^{-1}[9 + (16c^2 + 2c^4)y + 9y^2] \quad (18)$$

¹Where $g = \frac{(1-c^2)^2}{c} \tilde{g}$.

as expected. The high-field polynomials come from an expansion of the free energy F rather than the partition function \mathcal{Z} , so there is one further step.

We choose to consider $\frac{dF}{dy}$ for calculational convenience rather than directly taking the logarithm to obtain F , since the operation of taking a logarithm proved to be rather memory intensive. Since the free energy per site is defined as (absorbing a factor of $-\beta$)

$$F = \lim_{n \rightarrow \infty} \frac{1}{n} \log Z_n, \quad (19)$$

we can approximate this by

$$\frac{d}{dy} F \sim \frac{1}{n Z_n} \frac{dZ_n}{dy} \quad (20)$$

for some sufficiently large n (in our case we take $n = 32$). The behaviour observed for $\frac{dF}{dy}$ in [5] was in any case similar to that of F and M .

4 The Percolation Threshold on Φ^4 Graphs

Kazakov has already calculated the threshold on Φ^3 graphs, so it is a simple matter to repeat the calculation to obtain the result he stated ($p_{cr} = 2/3$), but did not derive, for Φ^4 graphs in [7]. We have chosen to work with Φ^4 graphs rather than Φ^3 graphs here because the expression for $g(z)$ turns out to be rather more inconvenient with Φ^3 graphs and reverting this in the manner of the previous section to get \mathcal{Z}_1 is much more cumbersome than it is for Φ^4 graphs.

The idea is to consider the percolation problem as the $q \rightarrow 1$ limit of a q -state Potts model, where the Potts partition function is

$$Z_{\text{Potts}} = \sum_{\{\sigma\}} \exp(-\tilde{\beta} \mathcal{H}). \quad (21)$$

with $\mathcal{H} = -\sum_{\langle ij \rangle} (\delta_{\sigma_i, \sigma_j} - 1)$, and the spins σ_i take on q values. This Potts partition function, just as in the Ising case, can be expressed as the matrix integral over $N \times N$ Hermitian matrices ϕ_i

$$F = \frac{1}{N^2} \log \int \prod_i \mathcal{D}\phi_i \exp(-S) \quad (22)$$

where

$$S = \frac{1}{2} \sum_{i=1}^q \phi_i^2 - \tilde{c} \sum_{i < j} \phi_i \phi_j - \frac{g}{4} \sum_{i=1}^q \phi_i^4. \quad (23)$$

and we have used $\tilde{c} = 1/(\exp(\tilde{\beta}) + q - 2)$ for the Potts coupling and temperature to distinguish them from the Ising case. The apparent factor of two difference between the $q = 2$ version of \tilde{c} and the Ising coupling in the previous section and the consequent factor of two in the temperature scales is accounted for by the use of a $\sigma_i \sigma_j$ interaction in the Ising model and a $\delta_{\sigma_i, \sigma_j}$ interaction in the Potts model.

This in turn may be recast into a matrix external field integral by introducing a further matrix integration in the dummy $N \times N$ Hermitian matrix X ,

$$F = \frac{1}{N^2} \log \int \mathcal{D}X \exp\left(-\frac{1}{2}X^2\right) \quad (24)$$

$$\times \left[\int \mathcal{D}\phi \exp\left(hX\phi - \frac{1+h^2}{2}\phi^2 + \frac{g}{4}\phi^4\right) \right]^q \quad (25)$$

where $h^2 = \tilde{c}$. In the limit $q \rightarrow 1$, the percolative probability $p = 1 - \exp(-\tilde{\beta})$ is related to these parameters by $h^2 = \tilde{c} = 1/p - 1$. The mean number of percolative clusters per unit volume $f(p)$ may be calculated from the quantity $\zeta(g, p)$, which is given in terms of the Potts free energy by

$$\lim_{q \rightarrow 1} \frac{\partial F}{\partial q} = \zeta(g, p). \quad (26)$$

Evaluating $\zeta(g, p)$ in the saddle-point approximation gives

$$\zeta(g, p) = \frac{1}{2N} \sum_{i=1}^N (x_i^*)^2 - \frac{2}{N^2} \log \Delta(x^*) - F^0(g), \quad (27)$$

where the x_i^* are the saddle point values of the X eigenvalues and $F^0(g)$ is the standard one-matrix model free energy. As in the Φ^3 model the $\frac{2}{N^2} \log \Delta(x^*)$ term is what counts for the percolative critical behaviour, and this gives

$$\begin{aligned} \frac{2}{N^2} \log \Delta(x^*) &= \int_{-a}^a \int_{-a}^a \rho(u) \rho(v) du dv \left[\log \left| \left(\frac{1}{p} - \frac{1}{2} \right) - \frac{1}{2}(u^2 + uv + v^2) \right| + \log |u - v| \right] \\ &- \frac{1}{2} \log \left(\frac{1}{p} - 1 \right), \end{aligned} \quad (28)$$

where ρ is the eigenvalue density for the one-matrix Φ^4 model which has support on $[-a, a]$. The Φ^4 model will be critical when the argument of the first logarithm is zero within the region of integration, which first occurs when $u^2 = uv = v^2 = a^2 = 2/3$, so $p_{cr} = 2/3$ as announced in [7]. Since $p_{cr} = 2/3 = 1 - \exp(-\tilde{\beta}_p)$, allowing for the factor of two between Ising and Potts conventions gives $\exp(-\tilde{\beta}_p) = \exp(-2\beta_p) = 1/3$, so on the Φ^4 graphs $u_p = \exp(-4\beta_p) = 1/9$ to be compared with the $1/4$ of the regular square lattice.

5 Padé Approximants for Φ^4 Graphs

The procedure is identical to the square lattice investigation: here we take Z_{32} , calculate

$$\frac{d}{dy} F \sim \frac{1}{32} \frac{dZ_{32}}{Z_{32} dy} \quad (29)$$

as our estimate of $\frac{d}{dy} F$ and then take unbiased Dlog-Padé approximants to this expression in order to determine y_c . Again, exact arithmetic is used until the final stage of extracting the zeroes and poles of the Padé approximant is reached.

Since our starting series is rather longer than the square lattice case, we calculate up to the $[15/15]$ approximant. In Fig. 3 we show the $[13/13]$, $[14/14]$ and $[15/15]$ approximants plotted against u . The near-diagonal approximants and lower approximants on the Φ^4 graphs which we also calculated all give very similar estimates for y_c and we have not shown them for clarity.

It is immediately obvious from Fig. 3 that although there is evidence for a change in the behaviour of the high-field series for $u > u_p$, it is rather less clear cut than for the square lattice series. We have emphasised the fact by plotting the $[7/7]$ square lattice approximant over the Φ^4 results to allow a direct comparison. Indeed, without the prejudice of a previous calculation of u_p it would be fair to state that although there are some signs of an increase in the estimates of y_c in the vicinity of $u_p = 1/9$ the variation is strongly apparent only for larger u values.

Our calculation of the series for Φ^4 graphs is for a set which includes various degeneracies such as self-energy and “setting-sun” diagrams in the ensemble of graphs, and the inclusion of such graphs has been found empirically to reduce finite-size effects [12] by comparison with more restricted ensembles of Φ^4 graphs. It is of course possible that *any* ensemble of random graphs may be subject to greater finite-size corrections than a square lattice so it is conceivable that this might explain a weaker signal for the Kertesz line than on the square lattice.

6 Conclusions

We reviewed the existing results for the existence of the Kertesz line for the Ising model on the square lattice, which lend support to the suggestion that a change in the behaviour of the high-field series should be visible around the percolation threshold. We then made use of the Boulatov and Kazakov solution of the Ising model on planar random graphs to construct a high-field series for planar Φ^4 graphs and subjected this to the same Dlog-Padé analysis carried out on the (shorter) square lattice series. We found that there are clear signs in this series too for a change in behaviour, since the estimated values of the radius of convergence, y_c , increase as $u = \exp(-4\beta)$ is increased, as seen in Fig. 3. What is less clear is the onset of this behaviour – there are no large jumps in the estimated y_c at u_p , such as occur for at least some of the approximants to the square lattice series. It is fair to say however, that all the plotted approximants (and others we have not plotted) do begin to increase around, or just above, the calculated value of u_p for the Φ^4 graphs, namely $1/9$.

On balance therefore, the analysis of the high-field series for the Ising model on planar Φ^4 random graphs also lends support to the existence of a Kertesz line. Since clusters of spins behave in the same manner on ensembles of planar random graphs as they do on the square lattice (the Wolff [13] or Swendsen-Wang [14] algorithms, for instance, still do an excellent job of reducing critical slowing down for Ising models on ensembles of random graphs) this is reassuring. It would have been interesting, but beyond the scope of the resources available to us, to extend the order of the Φ^4 high-field series to see what effect this had on the estimates of y_c . It would also be an interesting exercise to extend the

now vintage square lattice series for further comparison, bearing in mind that the clearest signal for a jump in y_c was only seen in the highest available approximants.

7 Acknowledgements

W.J. and D.J. were partially supported by EC IHP network “Discrete Random Geometries: From Solid State Physics to Quantum Gravity” *HPRN-CT-1999-000161*.

References

- [1] A. Coniglio and W. Klein, J. Phys. **A13** (1980) 2775.
- [2] C.M. Fortuin and P.W. Kasteleyn, Physica **57** (1972) 536.
- [3] M. Fisher, Physics **3** (1967) 255.
- [4] J. Kertesz, Physica **A161** (1989) 58.
- [5] J. Adler and D. Stauffer, Physica **A175** (1991) 222.
- [6] M. F. Sykes *et al.*, J. Math Phys. **6** (1965) 283; *ibid.* **14** (1973) 1066; J. Phys. **A6** (1973) 1498.
- [7] V.A. Kazakov, Phys. Lett. **A119** (1986) 140.
- [8] D.V. Boulatov and V.A. Kazakov, Phys. Lett. **B186** (1987) 379.
- [9] W. Janke, D. Johnston, and M. Stathakopoulos, Nucl. Phys. **B614** (2001) 494.
- [10] M. Staudacher, Nucl. Phys. **B336** (1990) 349.
- [11] J. Ambjorn, K. Anagnostopoulos, and U. Magnea, Mod. Phys. Lett. **A12** (1997) 1605; Nucl. Phys. (Proc. Suppl.) **63** (1998) 751.
- [12] J. Ambjorn, G. Thorleifsson, and M. Wexler, Nucl. Phys. **B439** (1995) 187; M.J. Bowick, S.M. Catterall, and G. Thorleifsson, Phys. Lett. **B391** (1997) 305.
- [13] U. Wolff, Phys. Rev. Lett. **62** (1989) 361.
- [14] R.H. Swendsen and J.-S. Wang, Phys. Rev. Lett. **58** (1987) 86.

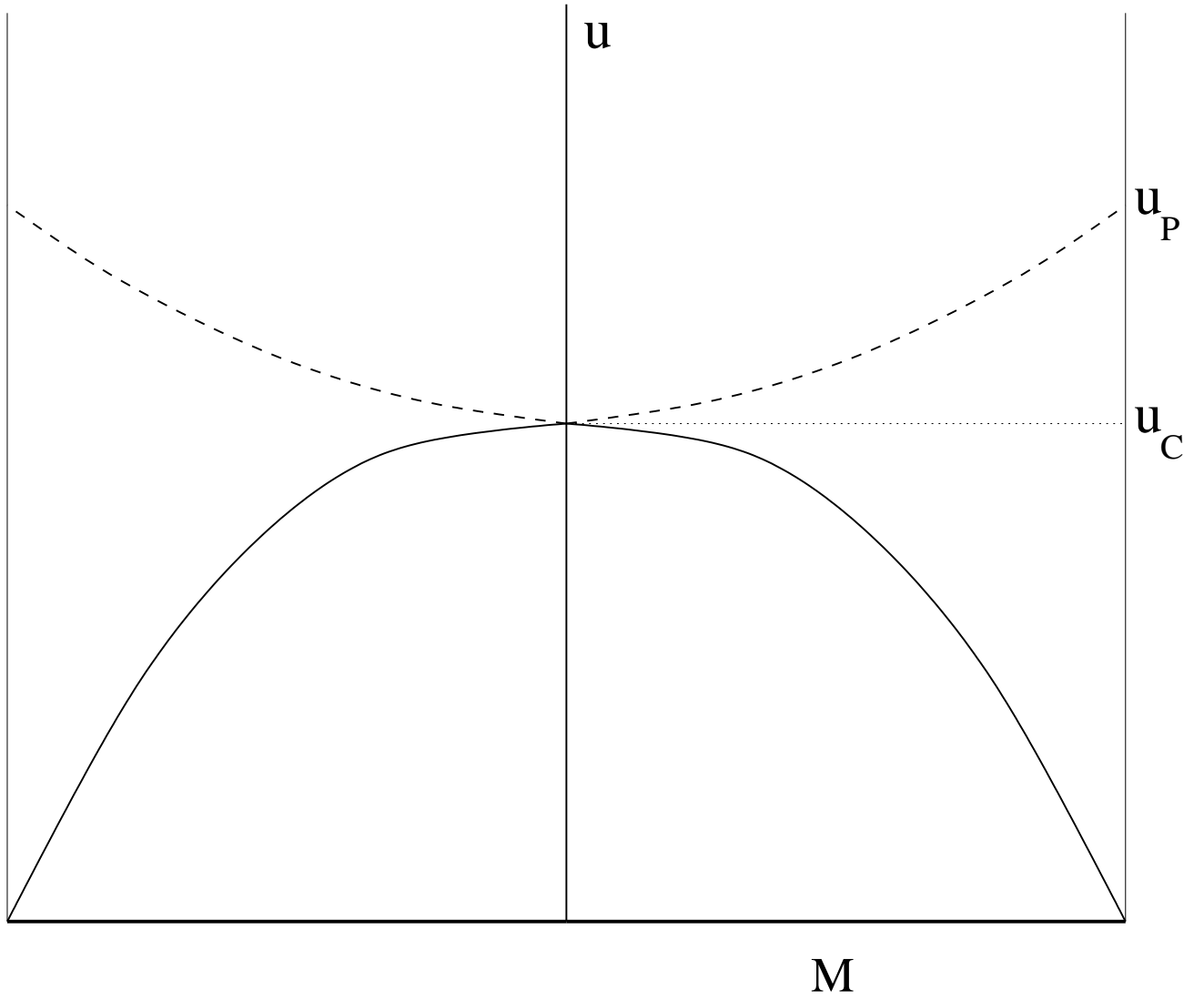


Figure 1: A schematic drawing of the Kertesz line in the $M, u = \exp(-4\beta)$ plane. The phase co-existence line is shown in bold, the Kertesz line dotted and the critical u_c and percolation u_p points are marked.

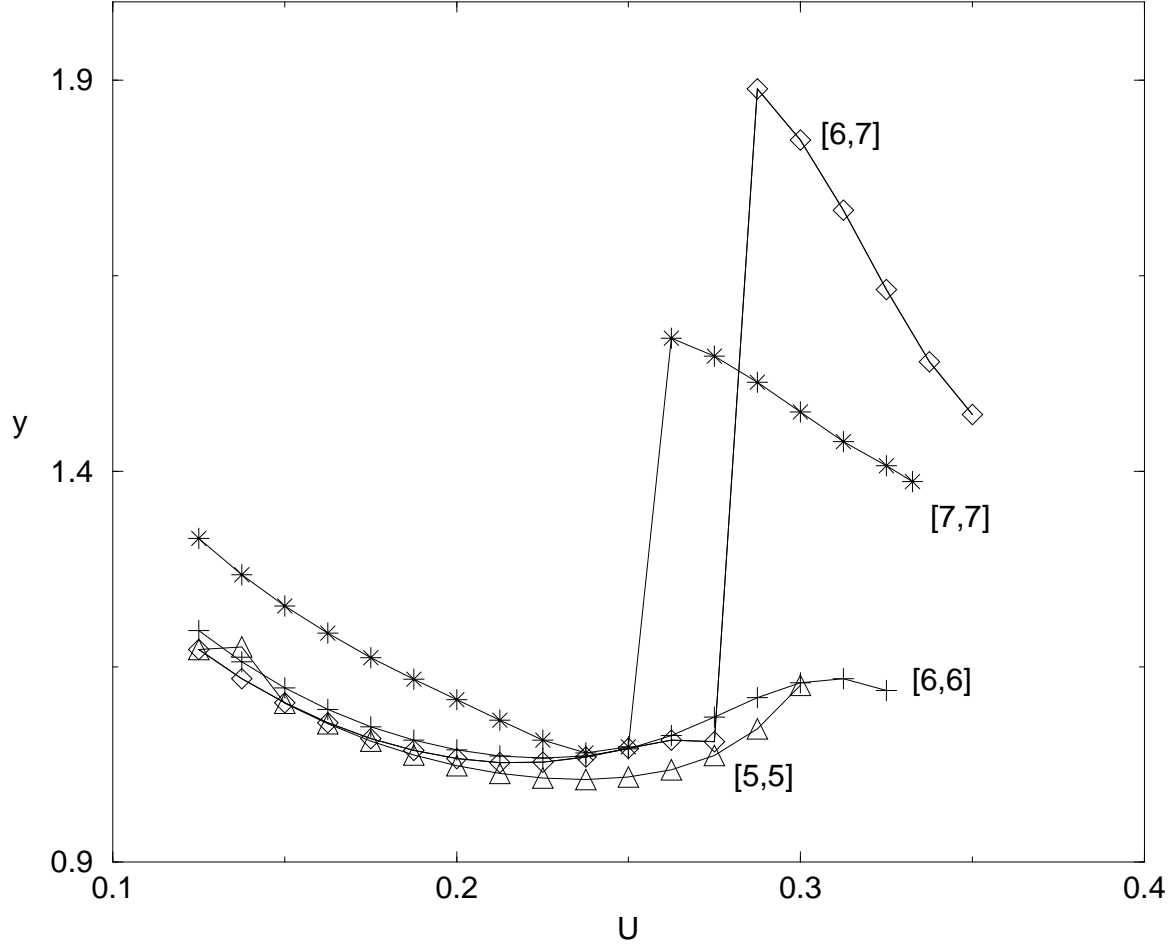


Figure 2: The estimated radius of convergence for the high-field series of $\frac{dF}{dy}$ on the square lattice plotted against u . The different symbols represent the different approximants used. Note that the jump is seen in both the [7/7] (star) and [6/7] (diamond) approximants, whereas the [6/6] (cross) and [5/5] (triangle) approximants give complex roots for some $u \sim u_p$.

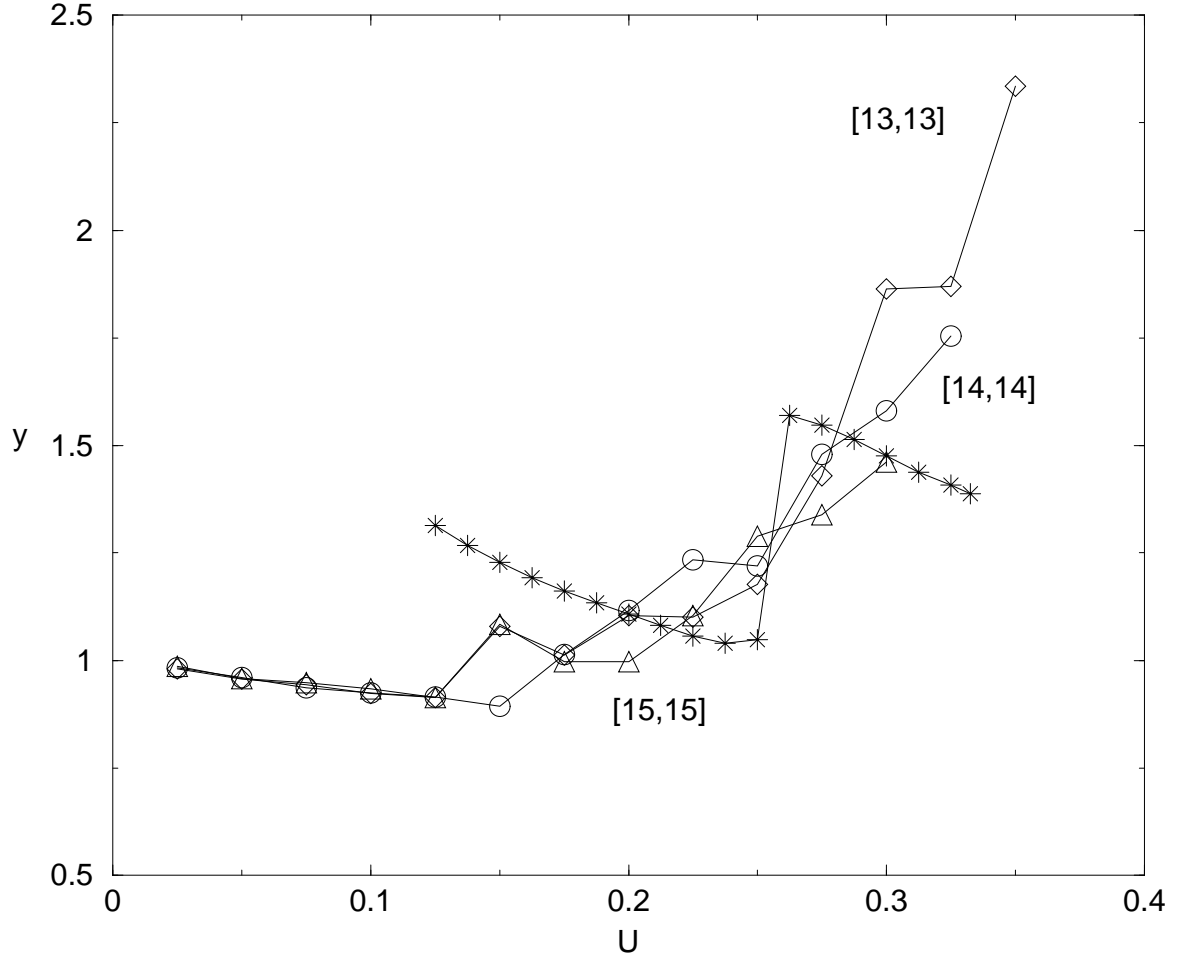


Figure 3: The estimated radius of convergence for the high-field series of $\frac{dF}{dy}$ on Φ^4 graphs plotted against u . The symbols are the estimates obtained from [13/13] (diamond), [14/14] (circle) and [15/15] (triangle) Padé approximants, and the [7/7] approximant for the square lattice is also shown for comparison using the starred symbol.